Vietnam Journal of Mechanics, VAST, Vol. 43, No. 2 (2021), pp. 183 – 196
DOI: https://doi.org/10.15625/0866-7136/15822

FAULT DIAGNOSIS OF ROLLING BEARINGS USING SINGULAR SPECTRUM ANALYSIS AND ARTIFICIAL NEURAL NETWORKS

Quang Thinh Tran[1], **Kieu Nhi Ngo**[2], **Sy Dzung Nguyen**[3,4,*]
[1]*Faculty of Mechanical Engineering, Industrial University of Ho Chi Minh City, Vietnam*
[2]*Ho Chi Minh City University of Technology, Vietnam*
[3]*Division of Computational Mechatronics, Institute for Computational Science, Ton Duc Thang University, Ho Chi Minh City, Vietnam*
[4]*Faculty of Electrical and Electronics Engineering, Ton Duc Thang University, Ho Chi Minh City, Vietnam*
[*]E-mail: nguyensydung@tdtu.edu.vn

Received: 06 January 2021 / Published online: 28 June 2021

Abstract. Singular spectrum analysis (SSA) has been employed effectively for analyzing in the time-frequency domain of time series. It can collaborate with data-driven models (DDMs) such as Artificial Neural Networks (ANN) to set up a powerful tool for mechanical fault diagnosis (MFD). However, to take advantage of SSA more effectively for MFD, quantifying the optimal component threshold in SSA should be addressed. Also, to exploit the managed mechanical system adaptively, the variation tendency of its physical parameters needs to be caught online. Here, we present a bearing fault diagnosis method (BFDM) based on ANN and SSA that targets these aspects. First, a multi-feature is built from pure mechanical properties distilled from the vibration signal of the system. Relied on SSA, the measured acceleration signal is analyzed to cancel the high-frequency noise. The remaining components take part in building a multi-feature to establish a database for training the ANN. Optimizing the number of the kept components is then carried out to obtain a dataset called Tr_Da. Based on Tr_Da, we receive the optimal ANN (OANN). In the next period, at each checking time, another database called Test_Da is set up online following the same way of building the Tr_Da. The compared result between the encoded output and the output of the OANN corresponding to the input to be Test_Da provides the bearing(s) health information. An experimental apparatus is built to evaluate the BFDM. The obtained results reflect the positive effects of the method.

Keywords: identifying bearing damage, AI for estimating damage, ANN-based damage identification, SSA for identifying damage.

1. INTRODUCTION

Mechanical systems always oscillate when operating. Although the vibrations can be described mathematically in many different ways, they are always influenced deeply by the external load as well as the mechanical properties such as the modulus of elasticity (E) and the polar moment of inertia of the cross-sectional area (I). For a specific system, in the case of unchanging in the external load, as a result, one can infer that there is a reduction of either E or I or both of them E and I if its vibration characteristics are changed. In general, such a growing down of E, or I, or EI, as above-mentioned, is seen as fault/damage. Therefore, to recognize the appearance of fault/damage on the mechanical system, one often exploits the variation of its vibration features. It is the theoretical basis of the well-known computational inverse techniques [1], by which MFDs based on DDMs or artificial intelligence (AI)-based DDMs are developed [2–6]. ANN, Fuzzy Logic (FL), and Adaptive Neuro-fuzzy Inference System (ANFIS) have been seen as useful AI tools for this approach [7–14]. To improve the ability to process, analyze, and extract valuable information from the mechanical vibration signal, SSA is also often employed [10, 11].

In [15], SSA was utilized to extract the bearing fault features. Based on the singular features selected from SSA, a continuous hidden Markov model was introduced. In [11], Nguyen et al. presented a method of health diagnosis of a mechanical structure upon ANFIS and SSA, in which SSA extracted vibration frequency-based information to set up databases, meanwhile ANFIS took the role of a classifier. In [16], another approach to the online assessment of bearing fault was depicted. Accordingly, SSA and sparse filtering were employed to establish a database, to which an ANFIS was employed to classify, label, and distill information about the object's health status. It can observe from the above-mentioned that SSA and data-driven models (DDMs), especially the AI-based models, are tools powerful and helpful to the fault diagnosis field. However, to exploit SSA more effectively for fault diagnosis, seeking a solution for quantifying the optimal component threshold in SSA analysis should be performed to enhance the capability to cancel the high-frequency noise. Also, to exploit the managed mechanical system adaptively, the variation tendency of its physical parameters needs to be caught online. These are our motivations for this research.

The aim of this paper is to presents a BFDM based on ANN and SSA. Firstly, a multi-feature is built from six pure mechanical properties deriving from the vibration signal of the system. Relied on SSA, the measured acceleration signal is analyzed to cancel the high-frequency noise. The remaining components take part in building the multi-feature to establish a database for training ANN. Optimizing the number of the kept components is then carried out to obtain a dataset called Tr_Da. The ANN is then employed to identify the dynamic response of the mechanical system corresponding to the bearing damage statuses reflected by the Tr_Da. In the next period, at each checking time, another database called Test_Da is set up online following the same way of building the Tr_Da. By employing Test_Da as the input of the ANN, the result from comparing between the encoded output and the output of the ANN provides information about the bearing fault status. The experimental system will be fitted up to verify the effectiveness of the method.

2. RELATED THEORY: SSA

SSA is a non-parametric technique of time series analysis upon the principles of multivariate statistics. It decomposes a given time series into a set of independent additive time series. Fundamentally, by using a procedure of principal component analysis, SSA projects the original time series onto a vector basis obtained from the series itself. The set of the series obtained from the decomposition can be interpreted as a slowly varying trend representing the signal mean at each instant, a set of periodic series, and aperiodic noise [11]. As a result, some information correlated with system response which is seen as features expressing the system attributes can be extracted [17–19].

In this study, the algorithm for SSA presented in [18,20] as below is used.

Step 1. Embedding

A given time series of N_0 data points $(z_1, z_2, \ldots, z_{N_0})$ is considered. From a selected window length $L, 1 < L < N_0$, one defines $K = N_0 - L + 1$ sliding vectors $\mathbf{X}_j = (z_j, z_{j+1}, \ldots, z_{j+L-1})^T, j = 1, \ldots, K$, and a trajectory matrix

$$\mathbf{X} = \begin{pmatrix} z_1 & z_2 & \cdots & \cdots & z_{N_0-L+1} \\ z_2 & z_3 & \cdots & \cdots & z_{N_0-L_0+2} \\ \vdots & \vdots & \ddots & \iddots & \vdots \\ z_{L-1} & z_L & \iddots & \ddots & z_{N_0-1} \\ z_L & z_{L+1} & \cdots & \cdots & z_{N_0} \end{pmatrix}. \tag{1}$$

Step 2. Singular value decomposition (SVD)

One firstly calculates the eigenvalues and eigenvectors of the matrix $\mathbf{S} = \mathbf{X}\mathbf{X}^T \in \Re^{L\times L}$. Let $\lambda_1, \ldots, \lambda_d$ be the non-zero eigenvalues of $\mathbf{S}$ arranged in the descending order, and $\mathbf{U}_1, \ldots, \mathbf{U}_d$ be the corresponding eigenvectors. Vectors $\mathbf{V}_i$ are then constructed, $\mathbf{V}_i = \mathbf{X}^T\mathbf{U}_i/\sqrt{\lambda_i}, i = 1, \ldots, d$. As a result, one obtains a decomposition of the trajectory matrix into a sum of matrices $\mathbf{X} = \sum_{i=1}^{d} \mathbf{E}_i$, where $\mathbf{E}_i = \sqrt{\lambda_i}\mathbf{U}_i\mathbf{V}_i^T$.

Step 3. Reconstruction

By applying a linear transformation known as diagonal averaging or Hankelization, each elementary matrix is transformed into a principal component of length N [20]. Let $\mathbf{Z} \in \Re^{L\times K}$ be a matrix of elements $z_{i,j}$. Then $\mathbf{Z}$ can be transformed into the reconstructed time series $g_1, g_2, \ldots, g_{N_0}$ as in (2), where, $L^* = \min(L, K)$, $K^* = \max(L, K)$.

$$g_k = \begin{cases} \dfrac{1}{k}\sum_{q=1}^{k} z_{q,k-q+1}, & 1 \le k < L^* \\ \dfrac{1}{L^*}\sum_{q=1}^{L^*} z_{q,k-q+1}, & L^* \le k \le K^* \\ \dfrac{1}{N_0-k+1}\sum_{q=k-K^*+1}^{N_0-K^*+1} z_{q,k-q+1}, & K^* < k \le N_0 \end{cases} \tag{2}$$

3. PROPOSED METHOD

3.1. Building database

3.1.1. *Setting up a multi-feature*

We establish a multi-feature (MF) from the acceleration signal measured from the oscillation of the mechanical system installing the managed bearings. The two required properties of a feature outlined in [21] are used here to check and select single features. They are the stability and dispersion properties. The stability one requires that if there is not any considerable change in the system's health status, then the variation range of the feature must be narrow. Conversely, if it is intense then the corresponding variation trend of the feature must be quickly but stably. While the dispersion attribute expresses the sensibility of the feature.

From the preprocessed acceleration signal $X(t_i)$, we set up the *MF* constituted of six single features as in (3), where t_i is the i-th sampled time, N is the number of sampling points.

The above single features consist of the mean value (MV), root mean square value (RMSV), maximum absolute value (MAV), square mean root value (SMRV), kurtosis coefficient (KC), and clearance factor (CF) [22]. The features of RMSV, MAV, and SMRV indicate the amplitude and energy over the time domain of the signal, while those of KC and CF reflect the distribution situation over the time domain. In the frequency domain, RMSF is a statistical feature describing the change in the frequency components to be extracted by power spectrum density analysis. $MF(k)$ denotes the multi-feature distilled from k-th vibration signal sample. By sliding a window with a width of N data points $X(t_i), i = 1, \ldots, N$, along with the time series, at its k-th position, we get the corresponding $MF(k)$.

$$MF(k) = \begin{bmatrix} X_{rmsv} = \left((1/N)\sum_{i=1}^{N} X^2(t_i)\right)^{0.5} \\ X_{mav} = \max\left(X(t_i)\right) \\ X_{smrv} = \left((1/N)\sum_{i=1}^{N} \sqrt{X(t_i)}\right)^{2} \\ X_{kc} = \left(1\Big/ {X_{rms}}^4\right)\sum_{i=1}^{N}\left(X(t_i) - (1/N)\sum_{k=1}^{N} X(t_k)\right)^4 \\ X_{cf} = X_{mav}/X_{rmsv} \\ X_{rmsf} = \left(\sum_{i=2}^{N}\dot{X}^2(t_i)\Big/ 4\pi^2\sum_{i=1}^{N} X^2(t_i)\right)^{0.5} \end{bmatrix}. \tag{3}$$

3.1.2. *Building database*

Building the input data space (IDS):

For each bearing damage status, a measured vibration data set is built corresponding to each case coming from H considered fault statuses. Thus, we have H original data sets signed as below

$$[\mathbf{D}_1, \mathbf{D}_2, \ldots, \mathbf{D}_H]^T. \tag{4}$$

Related to $\mathbf{D}_i$ which is corresponding to the i-th bearing fault type $(1 \leq i \leq H)$, by using SSA we get p time series signed

$$\left[\mathbf{D}_{i1}, \mathbf{D}_{i2}, \ldots, \mathbf{D}_{ip}\right], \quad i = 1, \ldots, H, \tag{5}$$

where p is a parameter selected by the designer. As mentioned in [11,18], the mechanical vibration signal is prone to the low-frequency range. Therefore, by putting the eigenvalues in the decreasing order, among the p subsets we delete $(p - q)$ last subsets which are considered as noise. Thus, we keep the first q subsets denoted as in (6) to build the training database.

$$\left[\mathbf{D}_{i1}, \mathbf{D}_{i2}, \ldots, \mathbf{D}_{iq}\right], \quad i = 1, \ldots, H. \tag{6}$$

It should be noted that p and q need to be optimized using an objective function reflecting the accuracy rate of the method (see Subsection 3.2).

For each time series in (6), for example $\mathbf{D}_{ij}$, $j = 1, \ldots, q$, we divided into P segments of the same size, based on $MF(k)$ as presented in (3), we obtain the feature distribution matrix signed $\mathbf{F}_{ij} \in \Re^{P \times k}$, $1 \leq k \leq 6$. By using this result for all the time series in (6), we formulate via a new data matrix $\bar{\mathbf{D}}_i$ as in (7) which is the input data space of the i-th data subset corresponding to the i-th bearing fault type.

$$\bar{\mathbf{D}}_i = \begin{bmatrix} \mathbf{F}_{i1} & \mathbf{F}_{i2} & \ldots & \mathbf{F}_{iq} \end{bmatrix} \in \Re^{P \times (kq)}, \quad 1 \leq k \leq 6. \tag{7}$$

Following this way for H the surveyed bearing fault types we establish an input data space in the form of matrix (8) for the two training dataset (Tr_Da) and test dataset (Test_Da).

$$\bar{\mathbf{D}} = \begin{pmatrix} f_{11} & f_{12} & \cdots & \cdots & f_{1(kq)} \\ f_{21} & f_{22} & \cdots & \cdots & f_{2(kq)} \\ \vdots & \vdots & \ddots & \iddots & \vdots \\ f_{(HP-1)1} & f_{(HP-1)2} & \iddots & \ddots & f_{(HP-1)(kq)} \\ f_{(HP)1} & f_{(HP)2} & \cdots & \cdots & f_{(HP)(kq)} \end{pmatrix} \in \Re^{(HP) \times (kq)}. \tag{8}$$

Building the output data space (ODS) and the databases:

The j-th fault type is encoded by a real number y_j. Thus, the output data space of the j-th subset can be depicted by vector $\bar{\mathbf{y}}_j$ of P elements y_j as in (9).

$$\bar{\mathbf{y}}_j = \left[y_j, \ldots, y_j\right]^T \in \Re^{P \times 1}, \quad j = 1, \ldots, H. \tag{9}$$

As a result, we gain the databases expressing the input-output relation in the Tr_Da and Test_Da as follows

$$\text{database} \equiv [\text{IDS} - \text{ODS}] \equiv [\bar{\mathbf{D}} - \bar{\mathbf{y}}], \tag{10}$$

where $\bar{\mathbf{D}} \in \Re^{(HP) \times (kq)}$ comes from (8) while $\bar{\mathbf{y}}$ is constituted of $\bar{\mathbf{y}}_i \in \Re^{P \times 1}$ in (9) as below

$$\bar{\mathbf{y}} = [\underbrace{y_1, \ldots, y_1}_{P}, \ldots, \underbrace{y_H, \ldots, y_H}_{P}]^T \in \Re^{(HP) \times 1}. \tag{11}$$

3.2. Estimating bearing fault status

Here, bearing(s) damage status is estimated following an ANN-based approach. Because a feedforward network with one hidden layer can handle most of the complex functions, in this study, a 3-layer feed-forward ANN as in Fig. 1 is chosen to train an identification model. The ANN is initialized by $N_I = kq$ neurons in the input layer, $N_H = 2kq$ neurons in the hidden layer, and $N_O = 1$ neuron in the output layer. Based on the training process, the number of neurons in the hidden layer N_H is then optimized to minimize the root mean square error (RMSE) between the prediction and data outputs. Any well-known training method can be employed for this aim. In this paper, the Levenberg–Marquardt algorithm is selected to update weight and bias values during the training progress and improve the convergence rate. By using the Tr_Da in the form of the database in (10) for training, we obtain an ANN that approximates the dynamic response of the mechanical system where the bearing(s) is installed.

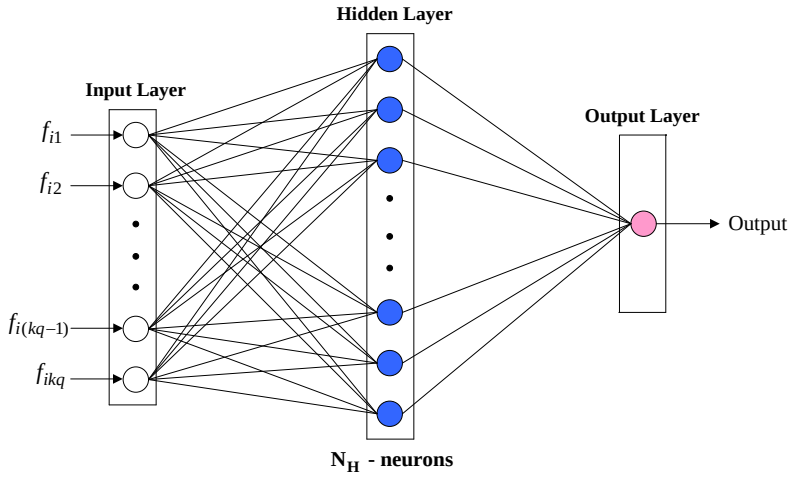

Fig. 1. Structure of the ANN

In fact, the two parameters p and q (signed p_{op}, q_{op}) in (5) and (8) need to be optimized to ensure the accuracy of the ANN-based approximation as above-mentioned. Be noted that p_{op}, q_{op} are understood as the values such that the fault diagnosis effectiveness of the BFDM is the best. So, if its efficiency of the BFDM is reflected by the mean accuracy (MeA) (13) then the objective function (12) can be used for this target.

$$J(p,q) = MeA(p,q) \to \max, \tag{12}$$

where

$$MeA(p,q) = 100 \times \sum_{i=1}^{H} true\_samples_n \Big/ \sum_{i=1}^{H} total\_samples_n(\%). \tag{13}$$

In (13), corresponding to the n-th damage type, $n = 1,\ldots,H$, $true\_samples_n$ is the number of checking samples expressing correctly the real status of the bearing, while $total\_samples_n$ is the total of checking samples used in the survey; H is the number of surveyed bearing fault types as mentioned in (4).

Fig. 2 shows the flowchart of the proposed algorithm. During the online bearing(s)'s health managing period, another dataset called Test_Da in the form of $\bar{\mathbf{D}}_i$ (7) is set up. By using the Test_Da as the input of the trained ANN we obtain its output $\hat{y}_i, i = 1, \ldots, P$. The compared error between $\hat{y}_i$ and the encoded output in (11) provides information about the health status. Namely, bearing status at the testing time is the one encoded by 'q' such that the condition as in (14) is satisfied.

$$\sum_{i=1}^{P} |\hat{y}_i - y_q| = \min_{h=1,\ldots,H} \sum_{i=1}^{P} |\hat{y}_i - y_h|. \tag{14}$$

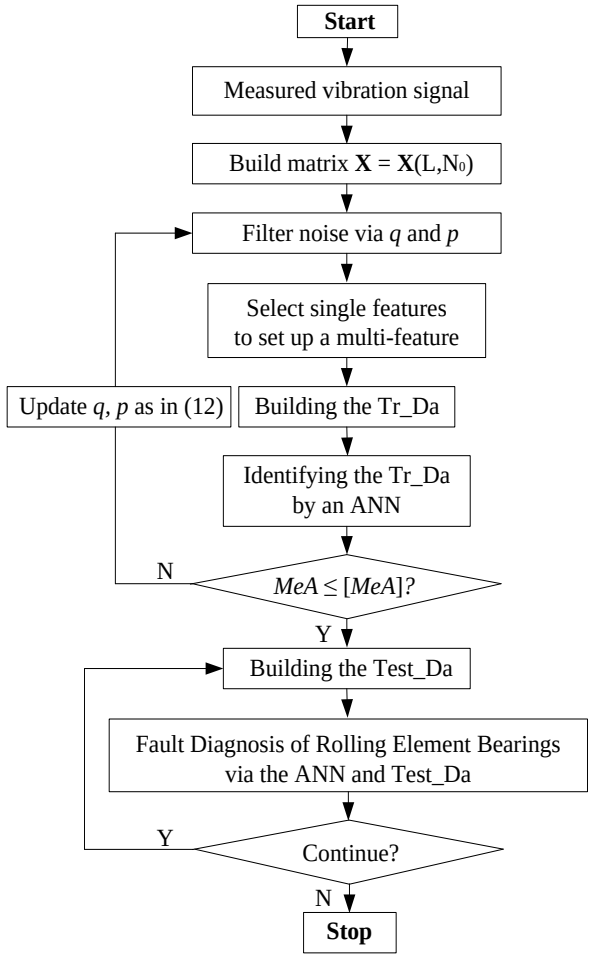

Fig. 2. Flowchart of the proposed method

4. VERIFYING THE METHOD

4.1. Description

In this section, we present the use of the BFDM for identifying the fault status of bearings. Two bearing vibration signal sources called Data Source 1 and Data Source 2 are employed here. Data Source 1 comes from the Western Reserve University bearing fault dataset while Data Source 2 derives from our experimental apparatus that will be detailed in Fig. 3. Along with *MeA* (13), the other parameters to be the percentage of correctly labeled samples (*Ac*) (15) and the root means square error (*RMSE*) (16) are also employed to evaluate the method.

$$Ac = 100 \times true\_samples_n / total\_samples_n(\%), \tag{15}$$

$$RMSE = \sqrt{\sum_{i=1}^{P} (y_i - \hat{y}_i)^2 \Big/ P}, \tag{16}$$

where, corresponding to the n-th damage type, $n = 1, \ldots, H$, $true\_samples_n$ is the number of checking samples expressing correctly the real status of the bearing; $total\_samples_n$ is the total of checking samples used in the survey; H is the number of surveyed bearing fault types as mentioned in (4); y_i and $\hat{y}_i$ respectively are encoding and predicting output.

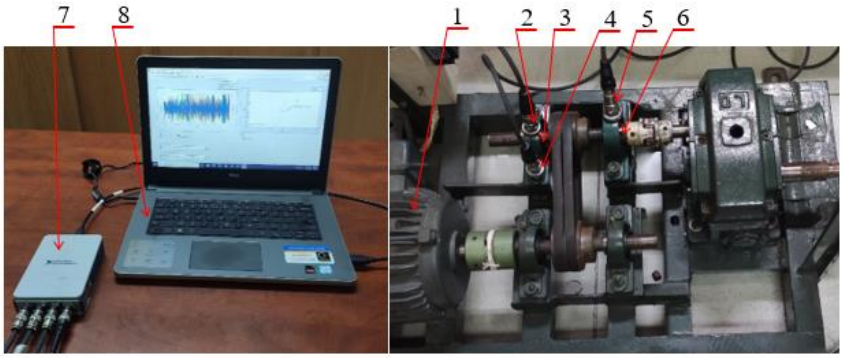

Fig. 3. Experimental apparatus for measuring vibration signal

4.2. Survey results

In this subsection, we show the results obtained from three surveyed cases detailed in Table 1. It is noted that in the table, 'Encoding value' is abbreviated to 'EV'. In all the cases, some other notations to be Ba, In, and Ou respectively express the Ball, or Inner or Outer of the surveyed bearing; NM shows the bearing to be undamaged; while and Lk = k HP, k = 1, 2.

Data Source 1:

We exploit the bearing-vibration data on '12k Drive End Bearing Fault Data', 'DE' (drive end accelerometer data), https://csegroups.case.edu/bearingdatacenter/pages/downloaddata-file. Some parameters are as follows: the fault diameter D1 = 0.014, and the motor load L1 = 1 HP.

Table 1. Three surveyed cases and the encoded values for expressing damage statuses

Case 1 - Data Source 1		Case 2 - Data Source 1		Case 3 - Data Source 2	
Status	EV (y_i)	Status	EV (y_i)	Status	EV (y_i)
NML0	0	NML1	0	NML0	0
BaD1L0	1	BaD1L1	1	BaD1L0	1
InD1L0	2	InD1L1	2	InD1L0	2
OuD1L0	3	OuD1L1	3	OuD1L0	3

Data Source 2:

Fig. 3 shows the experimental apparatus for measuring the vibration signal of the mechanical system used for surveys. In the apparatus, (1) is motor, (2), (4), and (5) are acceleration sensors, (3) and (6) are the surveyed bearings, (7) is the module for processing and transforming series vibration signal incorporate software-selectable AC/DC coupling (Model: NI-9234), while (8) is the computer for installing NI-9234 Driver as well as storing signal from the sensors. The single fault types of the bearings used for the surveys are detailed in Table 2.

Table 2. The single fault types used for surveys

Crack size		
Fault degrees and their location	Width (mm)	Depth (mm)
BaD1	0.15	0.2
InD1	0.2	0.3
OuD1	0.2	0.3

To estimate the effectiveness, the surveys using the proposed method along with two other methods were implemented. The first method was the one presented by Nguyen et al. (2013) in [10]. Related to this application, it should be noted that firstly we used the average quantity solution to wavelet transform coefficient (AQWTC) to build a database that reflects the dynamic response of the mechanical system described in Fig. 3 corresponding to all considered bearing damage statuses; the next steps were followed

Table 3. The compared results corresponding to each case as depicted in Table 1

Surveyed Cases	Mean accuracy (%)		
	[10]	[15]	Proposed (q_{ot})
Case 1	89.98	86.22	100
Case 2	91.65	98.08	100
Case 3	94.52	98.22	100

the BFDM. The second shown by Tao Liu et al. (2015) was Singular spectrum analysis and continuous hidden Markov model for rolling element bearing fault diagnosis shows in [15].

The obtained results are shown in Figs. 4–10 and Table 3. The results in Table 3 again show the positive role of the optimal value of q, as well as the compared effectiveness of the proposed method.

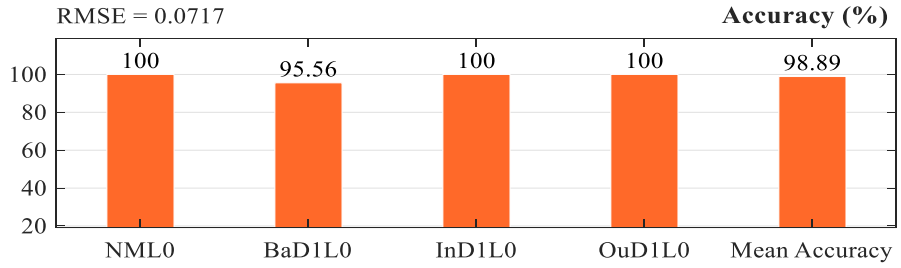

Fig. 4. The *Ac* (15) of the proposed BFDM in Case 1 (Table 1) when $q = 4$

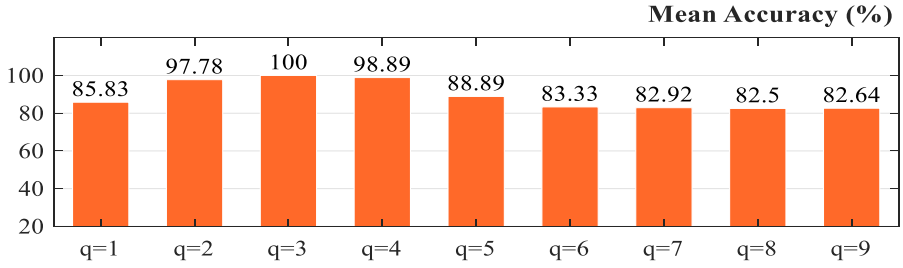

Fig. 5. The *MeA* (13) of the BFDM in Case 1 (Table 1) depends on q

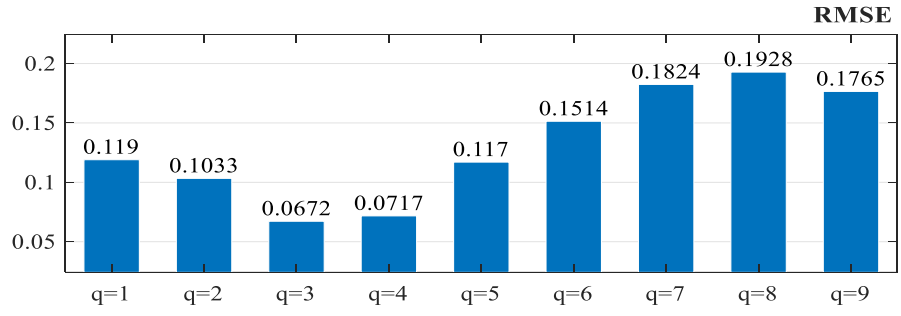

Fig. 6. The *RMSE* (16) of the BFDM in Case 1 (Table 1) depends on q

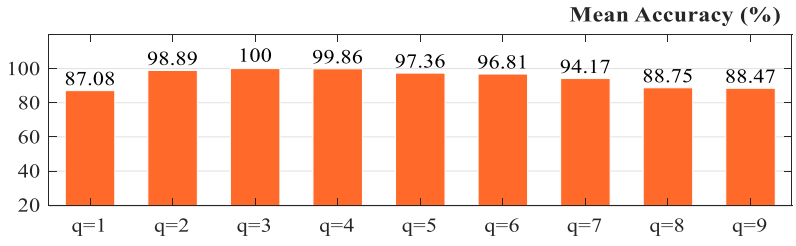

Fig. 7. The *MeA* of the BFDM in Case 2 (Table 1) depends on q

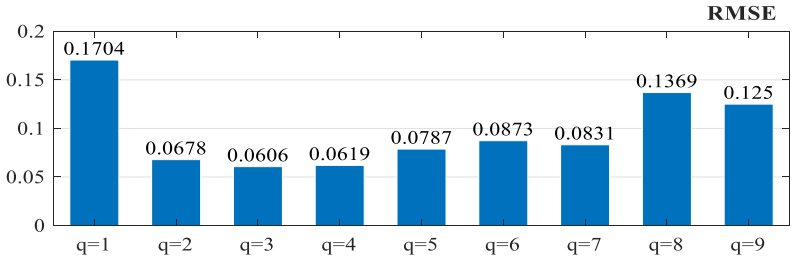

Fig. 8. The *RMSE* of the BFDM in Case 2 (Table 1) depends on q

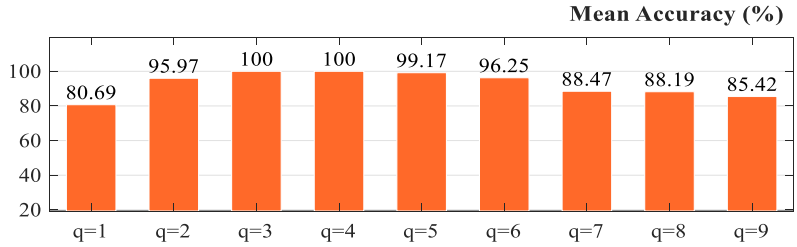

Fig. 9. The *MeA* of the proposed method in Case 3 (Table 1) depends on q

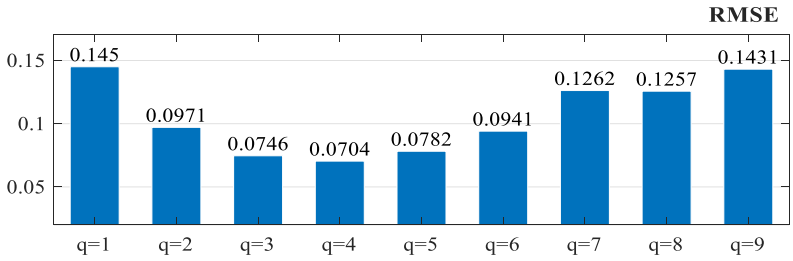

Fig. 10. The *RMSE* of the proposed method in Case 3 (Table 1) depends on q

4.3. Discussion

Three vital aspects that can be observed from the results shown in Figs. 4–10 are as follows. The first one is that the proposed BFDM can recognize reliably whether a fault existing in the bearings. In all of the databases, *Ac* (15) and *MeA* (13) are always high. Especially, it can get the highest to be 100% in some cases. The second one is that the effectiveness of the method depends significantly on the parameter q in Eq. (8). Therefore, an appropriate selection of the number of time series q is very critical. It is the necessary condition for minimizing the objective function (12). Let sign the optimal value of q to be q_{ot}, the third aspect relates to the stability of q_{ot} when changing the operating condition of the mechanical systems. Namely, in Case 1 and Case 2, both *Ac* and *MeA* could reach 100% as in Figs. 4–5 and 7 when q_{ot} is 3, while q_{ot} is 3 or 4 in Case 3 as in Fig. 9. It means we can select $q = 3$ for all cases in the two mechanical systems. However, this one is not an ensuring for other systems. To deal with this issue, we must find out q_{ot} when employing this method for a certain mechanical system under any its operating condition, then this optimal value can be used for all of other operating conditions.

Be noted that together with *Ac* and *MeA*, the *RMSE*s (16) in Figs. 6, 8, and 10 also reflect clearly the above aspects. Besides, the results in Fig. 4 illustrate that the method can identify fault reliably for either the balls or the inners or the outers of the bearings.

Taking part in the BFDM's effectiveness, along with the solution for quantifying the optimal number of time series q as above-mentioned, is the multi-feature (3). Constituted of the pure mechanical singular-features, based on the varying of EI, the multi-feature can distill well the meaningful information related to the health status of the bearings. The theoretical basis of this observation can be seen through the well-known finite element method. Obviously, in these surveys, a fault appearing on the bearing(s) makes the cross-sectional area of a certain element(s) belonging to the ball/inner/outer reduce, so its polar moment of inertia (I) grows down. As a result, as analyzed in Section 1, it then makes the system's vibration changed. Be noted that, faults related to the mechanical property in the form of the modulus of elasticity (E) also influence the system's dynamic response similarly. Such an attitude of the decline of EI is a vital direction for seeking singular features for the data-driven model-based fault identifications.

5. CONCLUSION

The BFDM for fault diagnosis of rolling element bearings based on SSA and ANN has been presented. This is the theoretical basis exploiting effectively the well-known computational inverse techniques. First, the multi-feature was built from six pure mechanical properties distilled from the system's vibration signal. Relied on SSA, the measured acceleration signal was analyzed to cancel the high-frequency noise. The remaining components took part in building the multi-feature to establish a database for training ANN. Optimizing the number of the kept components was then carried out to obtain Tr_Da, to which the ANN was optimized to get the OANN. Finally, bearing fault statuses could be identified by the OANN using the Test_Da in the online period. The survey results showed that the method could reflect the bearing health situations with a quite high accuracy, better than that from [10, 15].

ACKNOWLEDGMENT

The authors are very grateful to the reviewers for their useful comments and thoughtful suggestions to improve the paper. We would like to thank the Vietnam National Foundation for Science and Technology Development (NAFOSTED) under grant number 107.01-2019.328.

REFERENCES

[1] G. R. Liu and X. Han. *Computational Inverse Techniques in Nondestructive Evaluation*. CRC Press, (2003).

[2] A. Giantomassi, F. Ferracuti, S. Iarlori, G. Ippoliti, and S. Longhi. Electric Motor Fault Detection and Diagnosis by Kernel Density Estimation and Kullback–Leibler Divergence Based on Stator Current Measurements. *IEEE Transactions on Industrial Electronics*, **62**, (2015), pp. 1770–1780. https://doi.org/10.1109/tie.2014.2370936.

[3] Z. Gao, C. Cecati, and S. X. Ding. A Survey of Fault Diagnosis and Fault-Tolerant Techniques—Part I: Fault Diagnosis With Model-Based and Signal-Based Approaches. *IEEE Transactions on Industrial Electronics*, **62**, (2015), pp. 3757–3767. https://doi.org/10.1109/tie.2015.2417501.

[4] F. Filippetti, A. Bellini, and G. Capolino. Condition monitoring and diagnosis of rotor faults in induction machines: State of art and future perspectives. In *Workshop on Electrical Machines Design, Control and Diagnosis (WEMDCD)*, IEEE, (2013), https://doi.org/10.1109/WEMDCD.2013.6525180.

[5] J. Pons-Llinares, J. A. Antonino-Daviu, M. Riera-Guasp, S. B. Lee, T.-j. Kang, and C. Yang. Advanced Induction Motor Rotor Fault Diagnosis Via Continuous and Discrete Time–Frequency Tools. *IEEE Transactions on Industrial Electronics*, **62**, (2015), pp. 1791–1802. https://doi.org/10.1109/tie.2014.2355816.

[6] D. Z. Li, W. Wang, and F. Ismail. An Enhanced Bispectrum Technique With Auxiliary Frequency Injection for Induction Motor Health Condition Monitoring. *IEEE Transactions on Instrumentation and Measurement*, **64**, (2015), pp. 2679–2687. https://doi.org/10.1109/tim.2015.2419031.

[7] T. Boukra. Identifying new prognostic features for remaining useful life prediction using particle filtering and Neuro-Fuzzy System predictor. In *15th International Conference on Environment and Electrical Engineering (EEEIC)*, IEEE, (2015), https://doi.org/10.1109/eeeic.2015.7165399.

[8] T. Ince, S. Kiranyaz, L. Eren, M. Askar, and M. Gabbouj. Real-Time Motor Fault Detection by 1-D Convolutional Neural Networks. *IEEE Transactions on Industrial Electronics*, **63**, (2016), pp. 7067–7075. https://doi.org/10.1109/tie.2016.2582729.

[9] X. Dai and Z. Gao. From Model, Signal to Knowledge: A Data-Driven Perspective of Fault Detection and Diagnosis. *IEEE Transactions on Industrial Informatics*, **9**, (2013), pp. 2226–2238. https://doi.org/10.1109/tii.2013.2243743.

[10] S. D. Nguyen, K. N. Ngo, Q. T. Tran, and S.-B. Choi. A new method for beam-damage-diagnosis using adaptive fuzzy neural structure and wavelet analysis. *Mechanical Systems and Signal Processing*, **39**, (2013), pp. 181–194. https://doi.org/10.1016/j.ymssp.2013.03.023.

[11] S. D. Nguyen, Q. T. Tran, and K. N. Ngo. A fuzzy logic system built based on fuzzy data clustering and differential evolution for fault diagnosis. In *6th Asia Pacific Vibration Conference*, 24-26 November, HUST, Hanoi, Vietnam, (2015).

[12] S. D. Nguyen, Q. T. Tran, K. N. Ngo, X. P. Do, and S.-B. Choi. A structure damage detection method based on wavelet analysis and type-2 fuzzy logic system. In W.-H. Liao, editor, *Proceedings of the SPIE 9057, Active and Passive Smart Structures and Integrated Systems*, SPIE, (2014), https://doi.org/10.1117/12.2044642.

[13] S. Simani, S. Farsoni, and P. Castaldi. Fault Diagnosis of a Wind Turbine Benchmark via Identified Fuzzy Models. *IEEE Transactions on Industrial Electronics*, **62**, (2015), pp. 3775–3782. https://doi.org/10.1109/tie.2014.2364548.

[14] Y. Lei, F. Jia, J. Lin, S. Xing, and S. X. Ding. An intelligent fault diagnosis method using unsupervised feature learning towards mechanical big data. *IEEE Transactions on Industrial Electronics*, **63**, (2016), pp. 3137–3147. https://doi.org/10.1109/tie.2016.2519325.

[15] T. Liu, J. Chen, and G. Dong. Singular spectrum analysis and continuous hidden Markov model for rolling element bearing fault diagnosis. *Journal of Vibration and Control*, **21**, (2013), pp. 1506–1521. https://doi.org/10.1177/1077546313496833.

[16] Q. T. Tran, S. D. Nguyen, and T.-I. Seo. Algorithm for Estimating Online Bearing Fault Upon the Ability to Extract Meaningful Information From Big Data of Intelligent Structures. *IEEE Transactions on Industrial Electronics*, **66**, (2019), pp. 3804–3813. https://doi.org/10.1109/tie.2018.2847704.

[17] N. Golyandina, V. Nekrutkin, and A. Zhigljavsky. *Analysis of Time Series Structure*. Chapman and Hall/CRC, (2001).

[18] D. R. Salgado and F. J. Alonso. Tool wear detection in turning operations using singular spectrum analysis. *Journal of Materials Processing Technology*, **171**, (2006), pp. 451–458. https://doi.org/10.1016/j.jmatprotec.2005.08.005.

[19] B. Kilundu, P. Dehombreux, and X. Chiementin. Tool wear monitoring by machine learning techniques and singular spectrum analysis. *Mechanical Systems and Signal Processing*, **25**, (2011), pp. 400–415. https://doi.org/10.1016/j.ymssp.2010.07.014.

[20] F. J. Alonso and D. R. Salgado. Application of singular spectrum analysis to tool wear detection using sound signals. *Proceedings of the Institution of Mechanical Engineers, Part B: Journal of Engineering Manufacture*, **219**, (2005), pp. 703–710. https://doi.org/10.1243/095440505x32634.

[21] N. T. Truong, T.-I. Seo, and S. D. Nguyen. Bearing Fault Online Identification Based on ANFIS. *International Journal of Control, Automation and Systems*, **19**, (2021), pp. 1703–1714. https://doi.org/10.1007/s12555-020-0015-7.

[22] J. Wu, C. Wu, S. Cao, S. W. Or, C. Deng, and X. Shao. Degradation Data-Driven Time-To-Failure Prognostics Approach for Rolling Element Bearings in Electrical Machines. *IEEE Transactions on Industrial Electronics*, **66**, (2019), pp. 529–539. https://doi.org/10.1109/tie.2018.2811366.